Original Research

Extremely low-frequency electromagnetic fields induce neural differentiation in bone marrow derived mesenchymal stem cells

Hyun-Jung Kim, Jessica Jung, Jee-Hye Park, Jin-Hee Kim, Kyung-Nam Ko and Chan-Wha Kim

School of Life Sciences and Biotechnology, Korea University, Seoul 136-701, Korea
Corresponding author: Chan-Wha Kim. Email: cwkim@korea.ac.kr

Abstract

Extremely low-frequency electromagnetic fields (ELF-EMF) affect numerous biological functions such as gene expression, cell fate determination and even cell differentiation. To investigate the correlation between ELF-EMF exposure and differentiation, bone marrow derived mesenchymal stem cells (BM-MSCs) were subjected to a 50-Hz electromagnetic field during *in vitro* expansion. The influence of ELF-EMF on BM-MSCs was analysed by a range of different analytical methods to understand its role in the enhancement of neural differentiation. ELF-EMF exposure significantly decreased the rate of proliferation, which in turn caused an increase in neuronal differentiation. The ELF-EMF-treated cells showed increased levels of neuronal differentiation marker (MAP2), while early neuronal marker (Nestin) was down-regulated. In addition, eight differentially expressed proteins were detected in two-dimensional electrophoresis maps, and were identified using ESI-Q-TOF LC/MS/MS. Among them, ferritin light chain, thioredoxin-dependent peroxide reductase, and tubulin β-6 chain were up-regulated in the ELF-EMF-stimulated group. Ferritin and thioredoxin-dependent peroxide reductase are involved in a wide variety of functions, including Ca^{2+} regulation, which is a critical component of neurodegeneration. We also observed that the intracellular Ca^{2+} content was significantly elevated after ELF-EMF exposure, which strengthens the modulatory role of ferritin and thioredoxin-dependent peroxide reductase, during differentiation. Notably, western blot analysis indicated significantly increased expression of the ferritin light chain in the ELF-EMF-stimulated group (0.60 vs. 1.08; $P < 0.01$). These proteins may help understand the effect of ELF-EMF stimulation on BM-MSCs during neural differentiation and its potential use as a clinically therapeutic option for treating neurodegenerative diseases.

Keywords: Extremely low-frequency electromagnetic fields, BM-MSCs, neural differentiation, ferritin, Ca^{2+} regulation

***Experimental Biology and Medicine* 2013; 238: 923–931. DOI: 10.1177/1535370213497173**

Introduction

The discovery of non-invasive stimulation of the brain has given rise to a novel therapeutic target in cognitive psychology. Electrical stimulation has been used to treat progressive neurodegenerative disorders. Neurodegenerative diseases are characterized by progressive neuronal losses that affect specific regions of the nervous system. While advances in treatments for these illnesses have improved and elongated the life spans of the afflicted patients, no treatments for a complete cure are currently available. The impact of cellular therapy approaches that use stem cells to treat neurodegenerative disease has been tremendous but much is yet to be discovered. One potential therapy is the use of electromagnetic wave therapy on stem cells to induce them to differentiate into functional neuronal cells.

Mesenchymal stem cells (MSCs) have the capacity for self-renewal and exhibit multipotent differentiation potential through which they can produce connective tissues based on non-haematopoietic lineages. They are usually harvested from the bone marrow, adipose tissue and umbilical cord blood, among many other sources. MSCs possess several qualities that may be used to treat diseases of the central nervous system. They are known to secrete a variety of cytokines and growth factors that have both paracrine and autocrine activities against damaged tissues, including the brain.[1] MSCs are thought to have therapeutic potential because of their capacity for self-renewal and differentiation. They are also known to be able to restore injured neural tissues, a property that may afford promising treatments for neural injury. Previous studies showed that electromagnetic field radiation can modulate adult neurogenesis of the central nervous system and neuroendocrine functions.[2,3] It is also known that extremely low-frequency electromagnetic fields (ELF-EMF) enhance neuronal differentiation of cortical neural stem cells *in vitro* through the up-regulation of Ca_v1-channel expression and activity.[4]

The entry of Ca^{2+} through these channels can influence the transcription of certain classes of genes that are involved in cell survival and differentiation. The mechanism underlying the promotion of neural differentiation by ELF-EMF *in vitro* remains elusive. Therefore, we investigated the influence of ELF-EMF on the expression of proteins during the neural differentiation of BM-MSCs by using proteomic analysis.

Materials and methods

Cell culture and ELF-EMF stimulation

BM-MSCs (PT-2501, Walkersville Inc., MD) were thawed and cultured in Non-haematopoietic Expansion Medium (Miltenyi Biotec GmbH, Bergisch Gladbach, Germany) supplemented with 100 U/mL penicillin and 100 μg/mL streptomycin (Gibco BRL, Gaithersburg, MD, USA) in a humidified incubator at 37°C and 5% CO_2. Non-haematopoietic Expansion Medium was optimized and standardized for the reproducible and reliable expansion of MSCs.[5]

When the BM-MSCs were exposed to ELF-EMF, the medium was replaced with Dulbecco's Modified Eagle Medium Low Glucose (DMEM-LG, Gibco BRL, Gaithersburg, MD) supplemented with 10% foetal bovine serum (FBS, Lonza Walkersville Inc., MD, USA), 100 U/mL penicillin, and 100 μg/mL streptomycin (DMEM-LG, Gibco BRL, Gaithersburg, MD, USA), and the cells were incubated in a humidified incubator at 37°C and 5% CO_2. The BM-MSCs were cultured under an ELF-EMF at 50 Hz at 1 mT, and the control group was cultured without an ELF-EMF for 12 days. The cells were subjected to an ELF-EMF by using the device that was provided by Hankyong National University (Seoul, Korea).[6] After 6 days, the groups were subcultured to maintain their exponential growth. The BM-MSCs in the early passages (between four and seven passages) were used in all the experiments.

BrdU proliferation assay

The incorporation of BrdU (5-bromo-2′-deoxyuridine) during DNA synthesis was measured using a Cell Proliferation ELISA kit with BrdU (Roche Diagnostics, Penzberg, Germany) according to the manufacturer's protocol. Briefly, the cells were cultured on 96-well black plates to a density of 2000/well and exposed to 50 Hz, 1 mT ELF-EMF. The cells were pulse-labelled with BrdU for 24 h and fixed with FixDenat solution. Next, the BrdU label was located in the DNA using a peroxidase-conjugated anti-BrdU antibody (anti-BrdU-POD). The cells were then washed three times with washing solution. The bound anti-BrdU-POD was quantified with a peroxidase substrate (Luminol/4-iodophenol) in a luminometer. Each experiment was performed in triplicate.

Immunofluorescence staining

BM-MSCs were grown on glass cover slips and fixed in 4% paraformaldehyde (Fluka Chemie AG, Buchs, Switzerland) in PBS for 10 min. After three washes with cold PBS, the cells were permeabilized by immersion in 0.25% Triton X-100 in PBS for 10 min.[4] Next, the cells were incubated with 1% bovine serum albumin (BSA) at room temperature for 1 h to block non-specific binding of the antibodies. Staining was performed using 1 : 250 diluted mouse anti-MAP2 (Abcam, Cambridge, UK) and 1 : 40 diluted rabbit anti-Nestin antibodies (Santacruz, CA) in 1% BSA/PBS for 1 h followed by 1 : 200 diluted FITC-conjugated rabbit anti-mouse (green) and Texas Red-conjugated goat anti-rabbit (red) antibodies with three washes in cold PBS. Subsequently, the cells were stained with 4′,6-diamidino-2-phenylindole (DAPI DAPI, Sigma–Aldrich, MO, USA). After an additional three washes in cold PBS, the cells were mounted and viewed under a confocal laser scanning microscope that was equipped with an LSM 5 Exciter (Carl-Zeiss, Jena, Germany). Each experiment was performed in triplicate.

Intracellular calcium concentration

Fluo4-AM dissolved in DMSO was used for detecting intracellular Ca^{2+},[7] which bound to cytoplasmic-free Ca^{2+} and fluoresced green (peak at 516 nm). BM-MSCs were collected in polypropylene tubes and the pellets were obtained by centrifugation at 1300 rpm for 3 min. The cell pellets were re-suspended in the cell-loading medium at 10^5 cells/mL. The loading medium that was used in the experiments was Hank's Buffered salt solution (Invitrogen, Rockville, MD, USA) that consisted of 1 mM calcium, 1 mM magnesium, and 1% FBS. The cells were incubated with 2 μM Fluo4-AM at 37°C for 30 min in the dark. These cells were then washed three times with Dulbecco's Phosphate Buffered Saline (Invitrogen, Rockville, MD, USA) with no calcium and magnesium and incubated at 37°C for a further 30 min to allow for complete de-esterification of the dye by cytosolic esterases inside the cells. Subsequently, the cells were examined to determine their fluorescence of Ca^{2+} bound to Fluo4-AM using FL1 by FACS Calibur flow cytometry (BD Biosciences, San Diego, CA, USA). Simultaneously, they were treated with DMSO in parallel as a negative control for each treatment. The intensity of the fluorescence of the Fluo4-AM treated cells was normalized against the background of the DMSO-treated cells and the geometric mean value (Geo Mean) of the fluorescence for each experiment was calculated as the value of normalized Geo Mean using the program CellQuest (BD Biosciences, San Diego, CA, USA).[8]

Two-dimensional electrophoresis (2-DE)

Sample preparation for 2-DE. The BM-MSCs were exposed to 50 Hz, 1 mT ELF-EMF, and the control cells were harvested and washed twice in PBS. The pellets were obtained by centrifugation at 1300 rpm for 3 min. The lysates were extracted in 200 μL of radio-immunoprecipitation buffer that consisted of 50 mM Tris HCl (pH 8.0), 150 mM NaCl, 1% NP-40, 0.5% sodium deoxycholate, and 0.1% SDS, and centrifuged at 13,000 rpm and 4°C for 20 min. Then, the supernatant fractions were collected, and the cell debris was removed. The concentration of protein in each sample was determined by a modified Bradford protein assay method using BSA as a standard.[9]

Isoelectric focusing. Ready-to-use Immobiline DryStrips (24 cm, pH 4–7) were used for isoelectric focusing (IEF). DryStrips were re-hydrated with the samples (100 μg of protein) in 450 μL of solubilization solution that consisted of 8 M urea, 2% CHAPS, 1% IPG buffer (pH 4–7), 13 mM DTT, and a trace amount of BPB for 5 h without current and 5 h with current at 80 V. IEF was carried out using an IPGphor IEF system (AP Biotech, Sweden) at 200 V for 1 h, 500 V for 1 h, 100 V for 1 h, 1,000–8,000 V for 30 min, and constantly at 8,000 V until approximately 100,250 Vh was reached.[10] The gel strips were equilibrated over two steps of 10 min each with gentle shaking. The first equilibration solution contained 50 mM of pH 8.8 Tris-HCl buffer with 6 M urea, 20% glycerol, 2% SDS, and 1% DTT. In the second equilibration solution, the DTT was replaced with 2.5% IAA.

SDS-PAGE. After equilibration, the IPG strips were slightly rinsed with DW and blotted to remove the excess equilibration buffer. They were then applied onto 12% SDS-PAGE gels ($26 \times 20\,cm^2$) and overlaid with a solution of 0.5% agarose that consisted of a trace amount of BPB. 2-D SDS-PAGE was performed in an Ettan DALT II system (AP Biotech, Sweden) at 55 V for 1 h, 160 V for 1 h, and 330 V for 6 h.[10] Proteins were visualized by a silver staining method with some modifications.[11]

Image analysis. Computer analysis of the 2-DE image was carried out using ImageMaster™ 2D Platinum Software. The expression levels of the spots were determined by the volume of each spot divided by the total volume of all of the spots in the gel – a technique called Total Spot Volume Normalization. For each spot, the relative volume intensity was averaged and expressed as the mean ± standard error of the mean (SEM). The spots that were differentially expressed with a statistical difference were selected by using the Student's *t*-test ($P < 0.05$) and identified via liquid chromatography electrospray ionization tandem mass spectrometry (ESI-Q-TOF LC/MS/MS).

ESI-Q-TOF LC/MS/MS

In-gel digestion. The proteins were subjected to in-gel trypsin digestion.[12] The excised gel spots were destained with 100 μL of destain solution (30 mM potassium ferricyanide and 100 mM sodium thiosulfate) by shaking for 5 min. After removing the solution, the gel spots were incubated with 200 mM ammonium bicarbonate for 20 min. The gel pieces were then dehydrated with 100 μL of acetonitrile and dried in a vacuum centrifuge. Next, the dried gel pieces were re-hydrated with 20 μL of 50 mM ammonium bicarbonate that consisted of 0.2 μg of modified trypsin (Promega corporation, Madison, WI, USA) for 45 min on ice. After removing the solution, 30 μL of 50 mM ammonium bicarbonate was added. The digestion was performed overnight at 37°C. The peptide solution was desalted using a C18 nano column.

Desalting and concentration. Custom-made chromatographic columns were used for desalting and determining the concentration of the peptide mixture prior to mass spectrometric analysis.[5] A column consisting of 100–300 nL of Poros reverse phase R2 material (20–30 μm bead size, PerSeptive Biosystems, Framingham, MA, USA) was packed into a constricted GELoader tip (Eppendorf, Hamburg, Germany). A 10-mL syringe was used to force the liquid through the column by gently applying air pressure. Thirty microlitres of the peptide mixture from the digestion supernatant was diluted in 5% formic acid, loaded onto the column, and washed with 30 μL of 5% formic acid. For analyses by MS/MS, the peptides were eluted with 1.5 μL of 50% methanol/49% H_2O/1% formic acid directly into a pre-coated borosilicate nanoelectrospray needle (EconoTipTM, New Objective, USA).

ESI-Q-TOF LC/MS/MS

MS/MS of the peptides that were generated by in-gel digestion was performed by using a nano-ESI in a Q-TOF2 mass spectrometer (AB Sciex Instruments, CA).[11] The source temperature was room temperature. A potential of 1 kV was applied to the pre-coated borosilicate nanoelectrospray needles (EconoTipTM, New Objective, USA) in the ion source combined with a nitrogen back-pressure of 0–5 psi to produce a stable flow rate (10–30 nL/min). The cone voltage was 40 V. The quadrupole analyser was used to select precursor ions for fragmentation in the hexapole collision cell. The collision gas was Ar at a pressure of $6–7 \times 10^{-5}$ mbar, and the collision energy was 25–40 V. The product ions were analysed using an orthogonal TOF analyser that was fitted with a reflector, a microchannel plate detector, and a time-to-digital converter. The data were processed using a peptide sequencing system.

To identify the proteins, all the MS/MS spectra of the tryptic peptides that were derived from spots were compared against protein sequences from the NCBI database by using the MASCOT search program (www.matrixscience.com).

Western blotting. For western blotting, BM-MSCs lysate proteins (10 μg of control and 50-Hz ELF-EMF, $n = 3$, respectively) were denatured using SDS and incubated at 100°C for 5 min. Each protein sample was separated by 12% SDS-PAGE and transferred to nitrocellulose membranes (PALL Corporation, Ann Arbor, MI)) and then immunoblotted with ferritin antibody (Abcam, Cambridge, UK) and GAPDH (Abcam, Cambridge, UK), respectively.[13] The western blots were scanned using a flat-bed scanner and digitalized using Multi-Gauge v3.0 software (Fujifilm) and the values are mean ± standard error of the mean (SEM).

Statistical analysis

All the experiments were run in triplicate by using three independent observations per experiment. For 2-DE analysis, we collected individual samples from six control dishes and the 50 Hz, 1 mT ELF-EMF-treated dishes, respectively. For each of the spots, the relative intensity was averaged and expressed as mean ± SEM. All significant differences were assessed via unpaired Student's *t*-tests

(*$P < 0.05$, **$P < 0.01$, ***$P < 0.001$) using the SPSS 12.0 statistical software package (SPSS, Chicago, IL).

Results

BM-MSCs morphology and proliferation by ELF-EMF

A morphological study of the BM-MSCs that were cultured under ELF-EMF was performed at 2, 6 and 12 days after exposure. The unconditioned BM-MSCs had flattened, spindle-like, fibroblast-like features. The ELF-EMF-stimulated BM-MSCs-induced morphological changes that resembled neurite-like features (Figure 1(a)), which were narrow, elongated and branch-like in nature.

The proliferation of the BM-MSCs was estimated via a BrdU incorporation assay. Figure 1(b) shows that there was no significant difference among the cells treated with ELF-EMF on day 2, while those for days 6 and 12 showed a significant decrease in BrdU incorporation, and thus proliferation. This shows that ELF-EMF induced a positive effect on the differentiation of the BM-MSCs.

BM-MSCs neural differentiation by ELF-EMF

After ELF-EMF exposure for 12 days, the cells were detected as positive for mature neural marker nestin (Figure 2(a)). As shown in Figure 1(a), the cells cultured under ELF-EMF shows characteristic neuronal morphology consisting of a contracted cytoplasm, condensed nucleus and neurite-like outgrowths.

Figure 2(b) shows a fluorescence histogram; the fluorescence was shifted for the cells that were treated with ELF-EMF and their intracellular Ca^{2+} levels were increased. The BM-MSC intracellular Ca^{2+} content that was affected by ELF-EMF (269.17 ± 31.58) was elevated with statistical significance ($P < 0.05$) when compared with the control group (202.11 ± 33.73; Figure 2(c)). This result demonstrates a novel regulatory mechanism that employs intracellular Ca^{2+} signalling that is induced by ELF-EMF in BM-MSCs neural differentiation.

Comparative analysis of protein expression

Protein expression profiling experiments were conducted to identify proteins that the expressed proteins from the control BM-MSCs on the 2-DE gels were compared to those of ELF-EMF exposed cells for each of the six different gels. As depicted in Figure 3(a), approximately 1500 spots were detected in each of the gels through a pH range of 4–7 by image analysis.

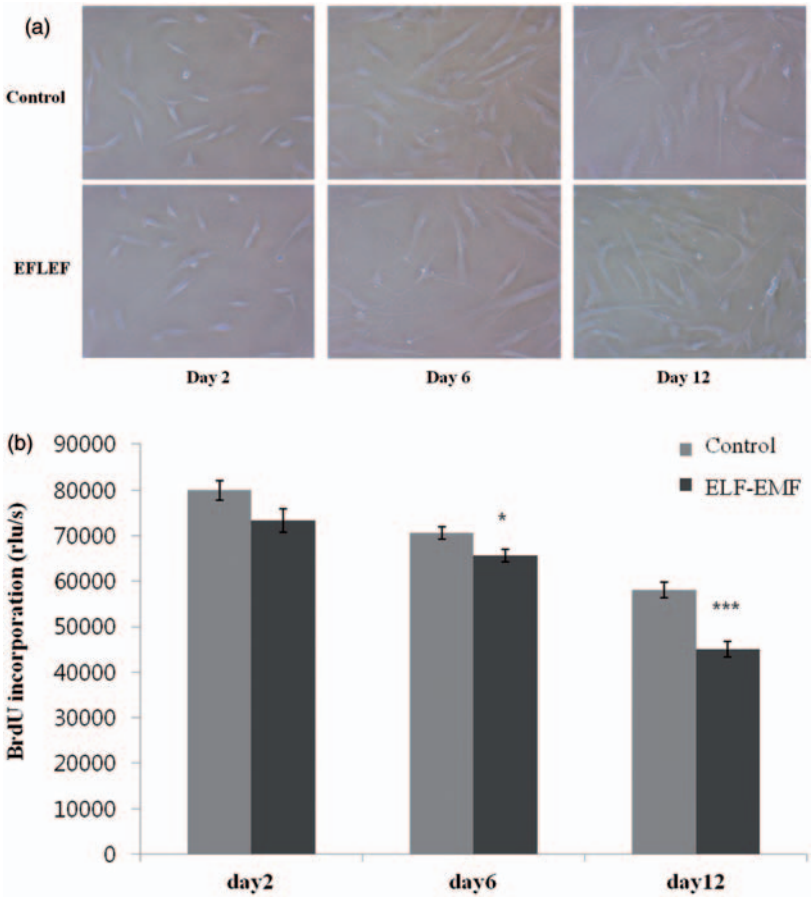

Figure 1 The morphology and proliferation of BM-MSCs during ELF-EMF exposure. Cells were cultured up to 12 days in DMEM-LG (with 10% FBS and 1% P/S) with or without ELF-EMF stimulation at 50 Hz, 1 mT. (a) Cell morphology of control group and ELF-EMF exposure group. Magnification: 100×. (b) Proliferative capacity was assessed through a BrdU incorporation assay after ELF-EMF exposure. The error bars represent the mean ± SEM. *$P < 0.05$; ***$P < 0.001$. (A color version of this figure is available in the online journal)

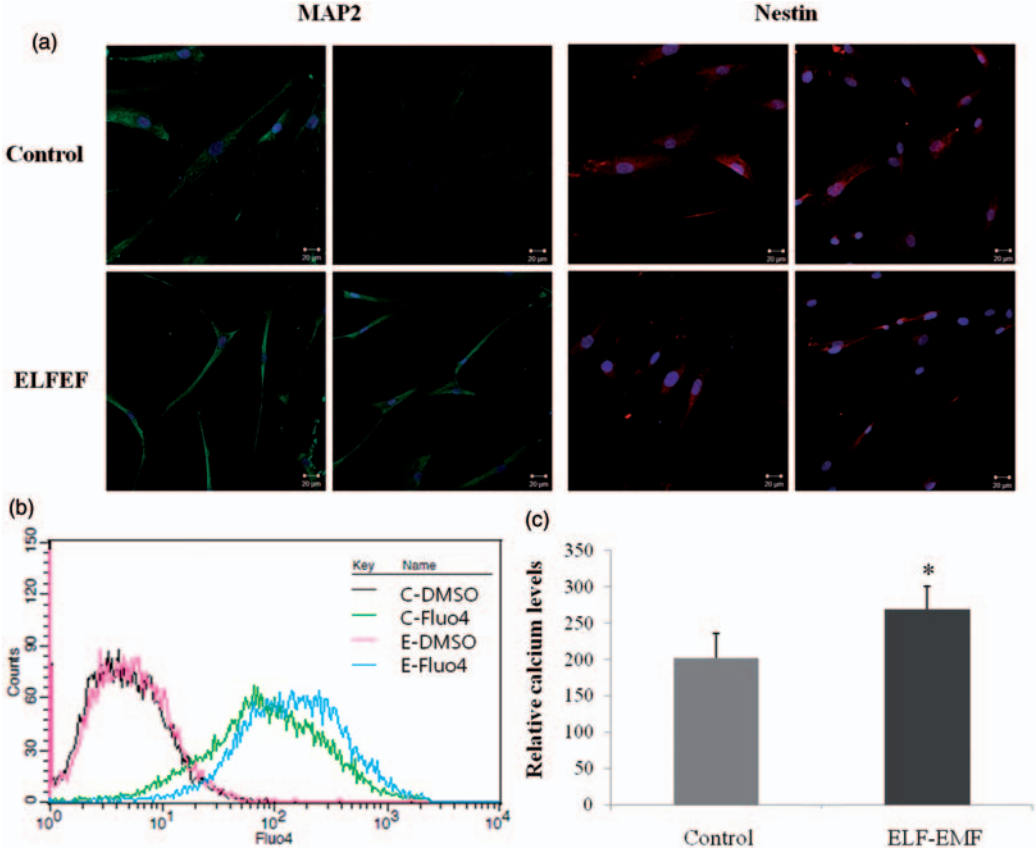

Figure 2 BM-MSCs neuronal differentiation after exposure to ELF-EMF. (a) Cells were stained with an antibody against MAP2 (green) and nestin (red). The top panel represents the control group where the four panels below show the cells that have undergone ELF-EMF treatment. In each experiment, the nuclei were counterstained with 4′,6-diamidino-2-phenylindole (DAPI) (blue). Magnification; 40×. (b) Intracellular Ca^{2+} contents measured with Fluo-4 AM in FACS, (c) Relative intracellular Ca^{2+} level compared to ELF-EMF group. Error bars represent mean ± SEM. *$P < 0.05$. (A color version of this figure is available in the online journal)

In the comparative analysis of the normalized volumes of each spot, eight spots were differentially expressed in the ELF-EMF-stimulated BM-MSCs (Figure 3(b)). Five spots were up-regulated by more than 200% and the other three were down-regulated by approximately 200% compared to the control group. The relative volume intensities of the up- and down-regulated spots are shown in Figure 3(b).

Identification of differentially expressed proteins

An ESI-Q-TOF LC/MS/MS analyser was used to obtain the data to identify the proteins accurately. The ESI-Q-TOF MS/MS spectrums were then matched against proteins in the NCBInr database by using the MASCOT program. Table 1 lists the proteins that were identified, which included five up-regulated proteins and three down-regulated proteins.

Western blot analysis of the ferritin light chain

To confirm the identity of protein deduced from the result of ESI-Q-TOF LC/MS/MS, the expression level of ferritin was analysed by Western blot (Figure 4). The total protein load was verified by the GAPDH expression level. Ferritin light chain expression in the ELF-EMF-stimulated group was significantly higher than that in the control group (0.60 vs. 1.08; $P < 0.05$).

Discussion

Many epidemiological surveys were conducted to study the biological effects of electromagnetic fields on humans.[14] In previous studies, electromagnetic radiation could be used to modulate adult neurogenesis as well as central nervous and neuroendocrine functions.[2,3] ELF-EMF enhance the neuronal differentiation of cortical neural stem cells *in vitro*.[4] Moreover, magnetic fields induce neurite outgrowth in chromaffin cells.[15] However, no study has systematically examined the effects of ELF-EMF at the cellular level.

In this study, we proposed the possibility of ELF-EMF having a positive effect on BM-MSC neural differentiation (Table 2). BM-MSC proliferation activity decreased when the cells were subjected to 50 Hz, 1 mT ELF-EMF compared with a control group of cells that were not exposed to ELF-EMF (Figure 1(b)). The decreased BM-MSC proliferation capacity under the influence of ELF-EMF suggests that ELF-EMF induces a positive effect on the differentiation of BM-MSCs. In addition, neural differentiation related mRNA levels were verified and shown to be increased as a result of 50 Hz, 1 mT ELF-EMF treatment (supplementary data). Notably, intracellular Ca^{2+} levels were elevated (Figure 2(b) and (c)) after ELF-EMF exposure. These results suggest that ELF-EMF enhance the neural differentiation of BM-MSCs.

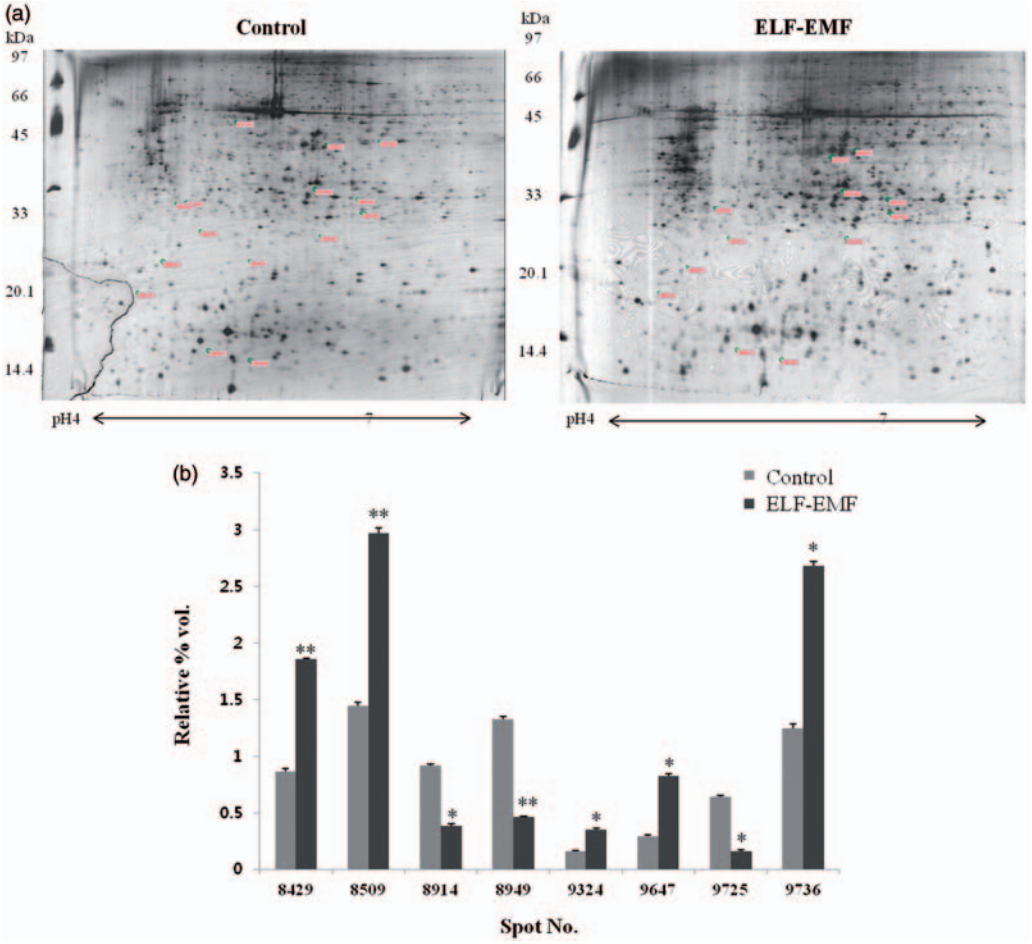

Figure 3 Representative 2-DE maps of whole-cell lysates of BM-MSCs and differentially expressed spots after ELF-EMF. A colour version of this figure is available in the online journal.Representative 2-DE maps of whole-cell lysates from BM-MSCs. Proteins totalling 100 μg were separated via 2-DE using a 24-cm pH 4–7 IPG strip and homogenous 12% SDS-PAGE. The map was analysed using the Image Master 2D Platinum Software (version 6.0, Amersham Biosciences). (a) 2-DE maps for control group and ELF-EMF-treatment group, (b) Differentially expressed, which is the average% volumes of the spots, for proteins that were two-fold up- and down-regulated between the control group and ELF-EMF group. Statistically significant spots are represented in the graph ($n = 6$). The error bars represent the mean ± SEM. *$P < 0.05$; **$P < 0.01$. (A color version of this figure is available in the online article)

Table 1 Identification of the up- and down-regulated proteins in the 50 Hz, 1 mT ELF-EMF-treated group by using ESI-Q-TOF-LC/MS/MS

Spot no.	Identification	MW (Da)	pI	Score*	Accession no.
Up-regulated					
8429	p24k-1 (AA 1-91)	10,109	8	61	CAA34498
8509	Thioredoxin-dependent peroxide reductase	28,017	7.67	92	NP_006784
9324	Ferritin light subunit	16,441	5.65	58	AAA52440
9647	Tubulin β-6 chain	50,281	4.77	47	Q9BUF5
9736	cytosolic inorganic pyrophosphatase	32,277	5.42	54	AAD24964
Down-regulated					
8914	Thioredoxin 2	18,515	8.45	39	AAF86467
8949	Thioredoxin 1	11,971	4.69	75	AAF86466
9725	*N*-acetyl-β-glucosaminidase prepro-polypeptide	64,720	7.03	40	AAA51828

*The score is $-10 \times \log(P)$, where P is the probability that the observed match was a random event. It was based on the data in the NCBInr database using the MASCOT search program for MS/MS data.

In the present study, to determine how ELF-EMF act at the cellular level, proteomic analysis of BM-MSCs with or without ELF-EMF exposure was performed to identify differentially expressed proteins that responded to ELF-EMF. Expression of the ferritin light subunit, tubulin β-6 chain, thioredoxin-dependent peroxide reductase, p24k-1, and cytosolic inorganic pyrophosphatase were shown to be up-regulated, and the expression of thioredoxin1, thioredoxin2, and *N*-acetyl-β-glucosaminidase prepro-polypeptide were shown to be down-regulated in BM-MSCs that

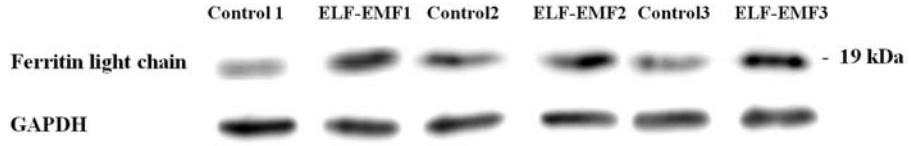

Figure 4 Western blot analysis of the ferritin light chain. Western blot analysis of hUC-MSCs lysate proteins (10 μg) from each set of the two groups was conducted. Quantitative analysis of the gel bands was conducted using Scion image analysis software (Scion Corp., MD) ($n = 3$, respectively)

Table 2 Summary of positive effects of ELFEF on the differentiation of BM-MSCs

	Control	EMF
Proliferation Rate	Normal rate	Decreased rate
Stemness markers (gene and protein expression)	High	Decreased
Differentiation markers (gene and protein level)	Low	High

had been exposed to 50 Hz, 1 mT ELF-EMF compared with the control group. We also confirmed the increase of calcium concentrations in response to ELF-EMF. The rapid increase of calcium ion is known to induce the production of ROS which results in apoptosis.[16] Prdx3 and ferritin are expected to be related in repressing the production of ROS. Prdx3, known as thioredoxin-dependent peroxide reductase, acts as anti-oxidant in mitochondria. Ferritin down-regulates the production of ROS caused by rapid increase of Fe ions.[17] These two protein play a significant role in repressing the production of ROS caused by surge of calcium ion.

Ferritin is an important regulator of intracellular iron content. Ferritin subunits consist of two types – a light chain and a heavy chain—which share extensive homology with each other. Pharmacologically obtained iron depletion induces major cellular alterations, including cell cycle arrest and apoptosis,[18] but at elevated tissue concentrations, iron is a potential toxin.[19] The storage of intracellular iron in ferritin molecules together with the down-modulation of the transferrin receptor are the two key mechanisms through which human tissues are shielded from the toxic effects of excess iron.[20] Ferritin can be viewed as both a storage pool of iron and as a site for cellular detoxification.[21] In several neurodegenerative disorders such as Alzheimer's disease and Parkinson's disease, ferritin subunit expression and brain iron homeostasis in general may be altered.[22]

Ferritin is also involved in calcium homeostasis. Ferritin, as the protein regulating the cellular iron levels, repressed the production of reactive oxygen species (ROS).[23] The synthesis of ferritin is regulated by the iron regulatory protein which also acts as an aconitase in TCA cycle converting citrate to isocitrate. The energy produced in the TCA cycle is used in actin filament reorganization involved in neural differentiation through neurite outgrowth.[17] Based on the hypothesis, we are currently researching on the signalling pathways relating ferritin to neural differentiation.

Thioredoxin-dependent peroxide reductase (Peroxiredoxins3, Prdx3) is a new family of thiol-specific peroxidases that rely on Trx as the hydrogen donor for the reduction of H_2O_2 and lipid hydroperoxides.[24,25] Prdx3 is exclusively present in the mitochondria.[26] Prdx3 expression can be induced in response to oxidant treatments. Further, antisense-mediated inhibition of Prdx3 expression sensitizes bovine aortic endothelial cells to oxidative challenges.[27] In this study we propose that ferritin and Prdx3 exhibited antioxidant functions against iron or free radicals and had a neuroprotective effect.[28,29]

Tubulin is the major constituent of microtubules. Microtubules are fundamental eukaryotic cell components that are involved in a wide variety of functions, including mitosis, transport of various organelles, maintenance of cellular morphology, and axonal transport in neurons.[30] Vertebrates have six functional genes for a-tubulin and at least six for b-tubulin.[30–34] Although all these tubulin varieties are not expressed in a single tissue, five distinct a-tubulin isotypes and five different b-tubulin isotypes are expressed in the brain, chiefly in the neurons.[35,36] Tubulin β-6, also known as neuron-specific β-III tubulin, is expressed in relatively differentiated neurons after their commitment. Therefore, ELF-EMF enhances the neural differentiation of BM-MSCs and possibly exhibits a neuroprotective effect via up-regulation of Prdx3 and ferritin expression.

In summary, the results of this study could provide useful information for understanding the mechanism of ELF-EMF stimulation, which has beneficial effects on various physiological functions in humans and animals. Although the details of the mechanism remain unclear, the proteins that were identified in this study could provide a better understanding of the mechanism by which ELF-EMF operates in terms of the neural differentiation of BM-MSCs. ELF-EMF might represent a clinically useful means for the treatment of neurodegenerative disorders.

Author contributions: HJ conducted cell culture, proliferation assay, immunofluorescence staining, Western blotting and manuscript writing. JHP and JHK performed two-dimensional electrophoresis and ESI-Q-TOF MS/MS, JJ conducted intracellular calcium level and KN conducted RT-PCR. CK was involved in the experimental design of the study, in the interpretation of the data and manuscript editing. All the authors declare that they have no competing interests.

FUNDING

This work was supported by the Pioneer Research Program of the National Research Foundation of Korea and was funded by the Ministry of Education, Science and Technology (2009-0082941).

Abbreviations

BM-MSC	bone marrow derived mesenchymal stem cell
BPB	bromophenol blue
BSA	bovine serum albumin
2-DE	two-dimensional electrophoresis
ELF-EMF	extremely low-frequency electromagnetic fields
FBS	foetal bovine serum
GAPDH	glyceraldehyde-3-phosphate dehydrogenase
IAA	iodoacetamide
IEF	isoelectric focusing
LC-ESI MS/MS	liquid chromatography electrospray ionization tandem mass spectrometry
MSCs	mesenchymal stem cells
PBS	phosphate buffered saline
SEM	standard error of the mean
SDS-PAGE	sodium dodecyl sulphate polyacrylamide electrophoresis
TBST	Tween-20

REFERENCES

1. Joyce N, Annett G, Wirthlin L, Olson S, Bauer G, Nolta JA. Mesenchymal stem cells for the treatment of neurodegenerative disease. *Regener Med* 2010;**5**:933–46
2. Arias-Carrion O, Verdugo-Diaz L, Feria-Velasco A, Millan-Aldaco D, Gutierrez AA, Hernandez-Cruz A, Drucker-Colín R. Neurogenesis in the subventricular zone following transcranial magnetic field stimulation and nigrostriatal lesions. *J Neurosci Res* 2004;**78**:16–28
3. Czeh B, Welt T, Fischer AK, Erhardt A, Schmitt W, Muller MB, Toschi N, Fuchs E, Keck ME. Chronic psychosocial stress and concomitant repetitive transcranial magnetic stimulation: effects on stress hormone levels and adult hippocampal neurogenesis. *Biol Psychiatry* 2002;**52**:1057–65
4. Piacentini R, Ripoli C, Mezzogori D, Azzena GB, Grassi C. Extremely low-frequency electromagnetic fields promote in vitro neurogenesis via upregulation of Ca(v)1-channel activity. *J Cell Physiol* 2008;**215**:129–39
5. Kim HJ, Ji BR, Kim JS, Lee HN, Ha DH, Kim CW. Proteomic analysis of proteins associated with cellular senescence by calorie restriction in mesenchymal stem cells. *In Vitro Cell Dev Biol Anim* 2012;**48**:186–95
6. Cho H, Seo YK, Yoon HH, Kim SC, Kim SM, Song KY, Partk JK. Neural stimulation on human bone marrow-derived mesenchymal stem cells by extremely low frequency electromagnetic fields. *Biotechnol Prog* 2012;**28**:1329–35
7. Gee KR, Brown KA, Chen WN, Bishop-Stewart J, Gray D, Johnson I. Chemical and physiological characterization of fluo-4 Ca(2+)-indicator dyes. *Cell Calcium* 2000;**27**:97–106
8. Yu YL, Chou RH, Chen LT, Shyu WC, Hsieh SC, Wu CS, Zeng HJ, Yeh SP, Yang DM, Hung SC, Hung MC. EZH2 regulates neuronal differentiation of mesenchymal stem cells through PIP5K1C-dependent calcium signaling. *J Biol Chem* 2011;**286**:9657–67
9. Bradford MM. A rapid and sensitive method for the quantitation of microgram quantities of protein utilizing the principle of protein-dye binding. *Anal Biochem* 1976;**72**:248–54
10. So EJ, Kim HJ, Kim CW. Proteomic analysis of human proximal tubular cells exposed to high glucose concentrations. *Proteomics Clin Appl* 2008;**2**:1118–26
11. Kim HJ, Cho EH, Yoo JH, Kim PK, Shin JS, Kim MR, Kim CW. Proteome analysis of serum from type 2 diabetics with nephropathy. *J Proteome Res* 2007;**6**:735–43
12. Shevchenko A, Wilm M, Vorm O, Mann M. Mass spectrometric sequencing of proteins silver-stained polyacrylamide gels. *Anal Chem* 1996;**68**:850–58
13. Han GY, Park SA, Kim JH, Lee EK, Kim HJ, Seo YK, Park JK, Kim CW. Effects of vibration on the proteome expression of anterior cruciate ligament cells. *Exp Biol Med* 2011;**236**:783–89
14. Repacholi MH, Greenebaum B. Interaction of static and extremely low frequency electric and magnetic fields with living systems: health effects and research needs. *Bioelectromagnetics* 1999;**20**:133–60
15. Hernandez-Hernandez H, Cruces-Solis H, Elias-Vinas D, Verdugo-Diaz L. Neurite outgrowth on chromaffin cells applying extremely low frequency magnetic fields by permanent magnets. *Arch Med Res* 2009;**40**:545–50
16. Brookes PS, Yoon Y, Robotham JL, Anders MW, Sheu SS. Calcium, ATP, and ROS: a mitochondrial love-hate triangle. *Am J Physiol Cell Physiol* 2004;**287**:C817–33
17. Arosio P, Levi S. Ferritin, iron homeostasis, and oxidative damage. *Free Radic Biol Med* 2002;**33**:457–63
18. Le NT, Richardson DR. The role of iron in cell cycle progression and the proliferation of neoplastic cells. *Biochim Biophys Acta* 2002;**1603**:31–46
19. Torti FM, Torti SV. Regulation of ferritin genes and protein. *Blood* 2002;**99**:3505–16
20. Harrison PM, Arosio P. The ferritins: molecular properties, iron storage function and cellular regulation. *Biochim Biophys Acta* 1996;**1275**:161–203
21. Hansen TM, Nielsen H, Bernth N, Moos T. Expression of ferritin protein and subunit mRNAs in normal and iron deficient rat brain. *Brain Res Mol Brain Res* 1999;**65**:186–97
22. Roskams AJ, Connor JR. Iron, transferrin, and ferritin in the rat brain during development and aging. *J Neurochem* 1994;**63**:709–16
23. Mackenzie EL, Tsuji Y. Elevated intracellular calcium increases ferritin H expression through an NFAT-independent post-transcriptional mechanism involving mRNA stabilization. *Biochem J* 2008;**411**:107–13
24. Chae HZ, Chung SJ, Rhee SG. Thioredoxin-dependent peroxide reductase from yeast. *J Biol Chem* 1994;**269**:27670–78
25. Chae HZ, Kang SW, Rhee SG. Isoforms of mammalian peroxiredoxin that reduce peroxides in presence of thioredoxin. *Methods Enzymol* 1999;**300**:219–26
26. Watabe S, Hiroi T, Yamamoto Y, Fujioka Y, Hasegawa H, Yago N, Takahashi SY. SP-22 is a thioredoxin-dependent peroxide reductase in mitochondria. *Eur J Biochem* 1997;**249**:52–60
27. Araki M, Nanri H, Ejima K, Murasato Y, Fujiwara T, Nakashima Y, Ikeda M. Antioxidant function of the mitochondrial protein SP-22 in the cardiovascular system. *J Biol Chem* 1999;**274**:2271–78
28. Hattori F, Murayama N, Noshita T, Oikawa S. Mitochondrial peroxiredoxin-3 protects hippocampal neurons from excitotoxic injury in vivo. *J Neurochem* 2003;**86**:860–68
29. Shi ZH, Nie G, Duan XL, Rouault T, Wu WS, Ning B, Zhang N, Chang YZ, Zhao BL. Neuroprotective mechanism of mitochondrial ferritin on 6-hydroxydopamine-induced dopaminergic cell damage: implication for neuroprotection in Parkinson's disease. *Antioxid Redox Signal* 2010;**13**:783–96
30. Villasante A, Wang D, Dobner P, Dolph P, Lewis SA, Cowan NJ. Six mouse alpha-tubulin mRNAs encode five distinct isotypes: testis-specific expression of two sister genes. *Mol Cell Biol* 1986;**6**:2409–19
31. Lewis SA, Lee MG, Cowan NJ. Five mouse tubulin isotypes and their regulated expression during development. *J Cell Biol* 1985;**101**:852–61
32. Sullivan KF. Structure and utilization of tubulin isotypes. *Annu Rev Cell Biol* 1988;**4**:687–716

33. Sullivan KF, Cleveland DW. Identification of conserved isotype-defining variable region sequences for four vertebrate beta tubulin polypeptide classes. *Proc Natl Acad Sci USA* 1986;**83**:4327–31
34. Wang D, Villasante A, Lewis SA, Cowan NJ. The mammalian beta-tubulin repertoire: hematopoietic expression of a novel, heterologous beta-tubulin isotype. *J Cell Biol* 1986;**103**:1903–10
35. Moura Neto V, Mallat M, Jeantet C, Prochiantz A. Microheterogeneity of tubulin proteins in neuronal and glial cells from the mouse brain in culture. *EMBO J* 1983;**2**:1243–48
36. Burgoyne RD, Cambraydeakin MA, Lewis SA, Sarkar S, Cowan NJ. Differential distribution of beta-tubulin isotypes in cerebellum. *EMBO J* 1988;**7**:2311–19

(Received November 13, 2012, Accepted April 8, 2013)